

Influence of guides on critical speeds of circular saws

S. Singhanian, P. Kumar, S. K. Gupta and M. Law*

Machine Tool Dynamics Laboratory
Department of Mechanical Engineering
Indian Institute of Technology Kanpur
Kanpur, U.P. 208016, India
*Email: mlaw@iitk.ac.in

Abstract. This paper investigates the influence of guides on the critical speeds of circular saws. Guides constrain the out-of-plane lateral motion of these rotating saws, and have a stabilizing effect by increasing the critical speeds, below which the rotating saw is stable. We present expanded analytical formulations in which guides are modelled as multiple discrete spring-damper elements approximating the distributed nature of the guide pad and saw interactions. We observe that for a given guide pad area, convergence analysis is necessary to understand how many discrete spring-damper elements are actually necessary to approximate the distributed nature of the guide-pad and saw interactions. Curiously, we observe that damping in the guides has no significant influence on the critical speed, and that it only changes the nature of frequency-speed characteristics of the rotating saw. We also find that critical speeds are sensitive to guides modelled with a distribution of discrete spring elements along the radial and/or circumferential directions. These observations suggest that more generalized formulations that model the guide pads as distributed spring-damper systems, rather than multiple discrete spring-damper elements, are necessary. We expect our findings to instruct and advise the placement of guides on rotating circular saws, such that a preferential increase in critical speeds can be obtained to make possible high speed and productivity circular sawing operations in the wood working and metal cutting industries concerned with circular sawing processes.

Keywords: Circular Saw, Guides, Critical Speeds Instability

1 Introduction

Circular sawing is a common cutting operation across the wood working and metal cutting industries. It involves feeding a rotating circular saw into the workpiece to cut logs, bars, and tubes to lengths of desired sections. To meet the demands on high productivity in these industries, circular saws are desired to be operated at high speeds allowing more material to be removed per unit time. However, when the saw is rotating, forward and backward travelling waves are generated. The natural frequencies of the backward travelling waves decrease with an increase in saw rotation speed, and the speed at which a natural frequency corresponding to a backward wave becomes zero is known as the critical speed [1]. When rotation speeds correspond to the critical speed, large amplitude vibrations appear, which can destroy the saw, the work material being cut, and the machine tool system. It is hence necessary to understand the factors governing critical speed instability, which is the focus of this paper.

Significant research attention across Industries and Academia has been paid on characterizing, predicting, and avoiding critical speeds. In some early seminal work,

Mote and Nieh [2], and Szymani and Mote [3] studied the vibrations and critical speeds of rotating circular saws. Contemporarily, as a means of increasing the critical speeds of saws, Iwan and Moeller [4] presented formulations for saws constrained by guides. Guides constrain the out-of-plane lateral motion of rotating flexible saws, and increase their critical speeds. Since these guides offer resistance to motion, and act as a transverse load, Schajer [1], Hutton et al. [5], and Lehmann and Hutton [6], all investigated the influence of guided saws, with guides modelled as lumped spring-elements. Hutton [5] observed that multiple guides were necessary to increase the critical speed. Though their [1, 5 - 6] formulations allowed for the possibility of incorporating multiple guides, they ignored the influence of damping, if any, offered by guides. Damping in guides was investigated by Mote [7], and he observed that, if not favourably positioned, guides promote instability. However, his analysis was for the case of a stationary saw subjected to a moving load, and not the case we are interested in – a rotating, and constrained saw.

Since guides are actually pads distributed over a sector area constraining the lateral out-of-plane motion of the rotating saw, they need to be modelled as distributed systems. However, all the earlier reported work [1, 5 - 7], modelled the guide as a spring lumped at the geometric center of the guide pad. Mohammadpanah and Hutton [8] were the first to investigate the distributed pad-saw interaction by modeling the guide as 16 linear springs distributed equally over the area of the guide pad. However, the effect of distributed damping in the guide was ignored. They also did not report on how many springs are sufficient to describe the distributed guide area, i.e. no convergence analysis of critical speeds to an increase in number of springs was presented.

This paper addresses the above two issues, i.e. understanding through systematic convergence studies, how many spring-damper systems are actually necessary to approximate the distributed pad-saw interaction, and understanding the role of damping in guides on the critical speeds of circular saws. To do so, we systematically modify the formulations for guided rotating circular saws, to include the possibility of incorporating multiple spring-damper systems. These modified formulations are presented in Section 2. Models are first numerically verified in Section 3 with results from a commercially available circular sawing stability code, CSAW[®] [9]. Verification is only provided for the undamped guide modelled as a single spring. Numerically verified models are then subjected to convergence analysis in Section 4, which includes discussions on the influence of damping on critical speeds, as well as discussion about the influence of modelling discrete spring-damper elements distributed radially, and circumferentially. The paper is concluded in Section 5.

2 Mathematical model for the critical speed of circular saws

A circular saw, laterally constrained by a guide pad, is modelled as a flexible disc with a clamped inner radius, r_i , outer radius, r_o , rotating with an angular velocity of Ω in the clockwise direction as shown in Fig. 1. Ignoring any external load, the governing equation of motion of the circular saw in the stationary frame of reference with a guide pad modelled as multiple spring-damper systems, distributed equally over the

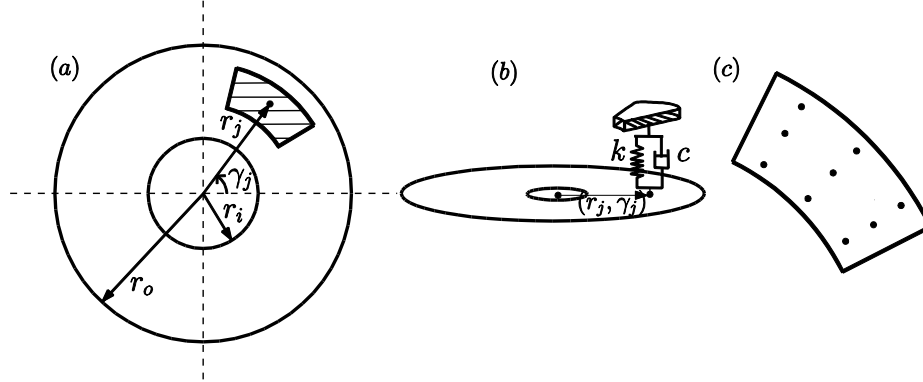


Fig. 1. Schematic of (a) circular saw and guide pad (b) the interaction between the guide pad and circular saw and (c) distribution of discrete spring-damper elements over the guide pad.

area of guide pad, is modified from [5] to become:

$$D\nabla^4 u + \rho h \left(\frac{\partial^2 u}{\partial t^2} + 2\Omega \frac{\partial^2 u}{\partial t \partial \gamma} + \Omega^2 \frac{\partial^2 u}{\partial \gamma^2} \right) - h \left[\left(\frac{1}{r} \right) \left(\frac{\partial}{\partial r} \right) \left(r \sigma_r \frac{\partial u}{\partial r} \right) + \left(\frac{1}{r^2} \right) \left(\frac{\partial}{\partial \gamma} \right) \left(\sigma_\gamma \frac{\partial u}{\partial \gamma} \right) \right] + \sum_{j=1}^J k_j u \left(\frac{1}{r} \right) \delta(r - r_j) \delta(\gamma - \gamma_j) + \sum_{j=1}^J c_j \frac{\partial u}{\partial t} \left(\frac{1}{r} \right) \delta(r - r_j) \delta(\gamma - \gamma_j) = 0 \quad (1)$$

wherein the first term represents bending stiffness, the second term represents inertial stress, the third term represents in-plane rotational stress, and the fourth and fifth terms represent stiffness and damping due to the interaction between the guide and circular saw, respectively at the location of r_j, γ_j .

In Eq. (1), D is the flexural rigidity ($= Eh^3/12(1 - \nu^2)$), E is the Young's modulus, h is circular saw thickness, ν is the Poisson ratio, ρ is the density of circular saw; $\nabla^4 \left(= \left[\frac{\partial^2}{\partial r^2} + \frac{1}{r} \frac{\partial}{\partial r} + \left(\frac{1}{r^2} \right) \left(\frac{\partial^2}{\partial \gamma^2} \right) \right]^2 \right)$ is a bi-harmonic operator; $\delta(\cdot)$ is the Dirac delta function, k and c represent the stiffness and damping of the guide pad; J is the number of spring-damper elements; $u(r, \gamma, t)$ is the transverse displacement of the circular saw, and r, γ represent the radial and angular coordinates with respect to a fixed frame of reference.

Eq. (1) is a fourth order partial differential equation, and since it is difficult to solve it analytically, we use the Galerkin projection method to solve it [5]. To represent the deflection of circular saw due to bending, the transverse displacement $u(r, \gamma, t)$ can be written by a modal expansion. Therefore, solution of the Eq. (1) is assumed in the following form [5, 10]:

$$u(r, \gamma, t) = \sum_{m=0}^m \sum_{n=0}^n [C_{mn}(t) \cos(n\gamma) + S_{mn}(t) \sin(n\gamma)] R_{mn}(r) \quad (2)$$

wherein $C_{mn}(t)$ and $S_{mn}(t)$ are the unknown functions (modal coordinates), m and n represent the number of nodal circles and nodal diameters, respectively, and $R_{mn}(r)$ are radial functions chosen to satisfy the inner and outer boundary conditions of the circular saw. These $R_{mn}(r)$ can be approximated by polynomial functions as [5]:

$$R_{mn}(r) = \sum_{i=0}^4 E_{mni} r^{m+i}, \quad (3)$$

wherein E_{mni} are unknown coefficients determined from the out of plane boundary conditions given by Eq. (4) and additional normalizing conditions, $R_{mn}(r_o) = 1$. Since the circular saw is clamped at its inner radius and is free at its outer radius, displacement and the slope at the inner radius will be zero whereas bending moment and shear force at the outer radius will be zero. Therefore, the boundary condition at the inner and outer radius in terms of transverse displacement can be written as:

$$\left. \begin{aligned} u(r_i, \gamma, t) = 0, \quad \frac{\partial}{\partial r} u(r_i, \gamma, t) = 0, \\ M_{rr}(r_o, \gamma, t) = 0, \quad Q_r(r_o, \gamma, t) - \frac{1}{r_o} \left(\frac{\partial}{\partial \gamma} \right) M_{r\gamma}(r_o, \gamma, t) = 0, \end{aligned} \right\} \quad (4)$$

wherein M_{rr} and $M_{r\gamma}$ are bending moments, and Q_r is the shear force [5]. Eq. (1) can be rewritten with brevity, in terms of a differential operator (L) as:

$$L(u) = 0, \quad (5)$$

wherein $L = D\nabla^4 + \rho h \left(\frac{\partial^2}{\partial t^2} + 2\Omega \frac{\partial^2}{\partial t \partial \gamma} + \Omega^2 \frac{\partial^2}{\partial \gamma^2} \right) - h \left[\left(\frac{1}{r} \right) \left(\frac{\partial}{\partial r} \right) \left(r \sigma_r \frac{\partial}{\partial r} \right) + \left(\frac{1}{r^2} \right) \left(\frac{\partial}{\partial \gamma} \right) \left(\sigma_\gamma \frac{\partial}{\partial \gamma} \right) \right] + \sum_{j=1}^J k_j \left(\frac{1}{r} \right) \delta(r - r_j) \delta(\gamma - \gamma_j) + \sum_{j=1}^J c_j \frac{\partial}{\partial t} \left(\frac{1}{r} \right) \delta(r - r_j) \delta(\gamma - \gamma_j)$.

Since the assumed form of the solution does not satisfy the equation of motion exactly, the residue can be minimised using the Galerkin projection approach, resulting in:

$$\int_0^{2\pi} \int_{r_i}^{r_o} L(u) (R_{ql} \cos(l\gamma)) r dr d\gamma = 0, \quad (6)$$

$$\int_0^{2\pi} \int_{r_i}^{r_o} L(u) (R_{ql} \sin(l\gamma)) r dr d\gamma = 0, \quad (7)$$

wherein $q = 0, 1, \dots, m, l = 0, 1, \dots, n$. Solving and simplifying Eqs. (6) and (7), we get:

$$\sum_{m=0}^m \alpha_1 \left[\delta_{qml}^{(1)} \frac{d^2 C_{ml}}{dt^2} + \delta_{qml}^{(2)} \frac{d S_{ml}}{dt} + \delta_{qml}^{(3)} C_{ml} \right] + \sum_{m=0}^m [N_{qml}^{(1)} C_{ml} + N_{qml}^{(2)} S_{ml}] = 0, \quad (8)$$

$$\sum_{m=0}^m \beta_1 \left[\delta_{qml}^{(1)} \frac{d^2 S_{ml}}{dt^2} - \delta_{qml}^{(2)} \frac{d C_{ml}}{dt} + \delta_{qml}^{(3)} S_{ml} \right] + \sum_{m=0}^m [N_{qml}^{(3)} C_{ml} + N_{qml}^{(4)} S_{ml}] = 0, \quad (9)$$

$$\alpha_1 = \begin{cases} \pi, & l \neq 0 \\ 2\pi, & l = 0 \end{cases}, \beta_1 = \begin{cases} \pi, & l \neq 0 \\ 2\pi, & l = 0 \end{cases}.$$

For the sake of brevity, $\delta_{qml}^{(1)}, N_{qml}^{(1)}, N_{qml}^{(2)}, N_{qml}^{(3)}, N_{qml}^{(4)}, \delta_{qml}^{(2)}, \delta_{qml}^{(3)}$ are not defined here, and the reader is directed to [5] for details. The above Eqs. (8) and (9) can be rewritten in a compact form as:

$$[A]\{\ddot{x}\} + [B]\{\dot{x}\} + [C]\{x\} = 0 \quad (10)$$

where the vector $\{x\}$ is an array of $\{C_{0,0}, C_{0,1}, \dots, C_{1,0}, C_{1,1}, \dots, C_{m,n}, S_{0,1}, S_{0,2}, \dots, S_{1,1}, S_{1,2}, \dots, S_{m,n}\}$. In the Eq. (10), $[A]$ is the mass matrix, $[B]$ is the gyroscopic matrix, and $[C]$ is the stiffness matrix. Since $[B]$ and $[C]$ depend on the rotational speed of circular saw, dynamics of circular saw depends on rotational speed. As Eq. (10) is a second order

linear differential equation, the solution of the equation can be assumed in the form of, $x(t) = \{X\}e^{\lambda t}$. On substituting the assumed form of the solution, Eq. (10) forms an eigenvalue problem which can be solved for every combination of rotational speed and other parameters. The imaginary part of the eigenvalue, λ of this eigenvalue problem corresponds to a natural frequency of the circular saw. To reduce the effective number of parameters, we non-dimensionalize Eq. (10) as:

$$\Omega_0 = \left[\frac{\rho h r_o^4}{D} \right]^{\frac{1}{2}} \Omega, \quad \zeta = k \left(\frac{r_o^2}{D} \right), \quad \phi = \left[\frac{\rho h r_o^4}{D} \right]^{\frac{1}{2}} \omega, \quad c_1 = \frac{c r_o^2}{\sqrt{\rho h r_o^4 D}}$$

wherein c_1 is the non-dimensional damping, ζ is the non-dimensional stiffness, ω is the natural frequency, ϕ is the non-dimensional natural frequency, and Ω_0 is the non-dimensional rotational speed.

We solve the above set of equations, and, at first verify the formulations against results from CSAW[®], as discussed next, in Section 3, followed by convergence testing, and investigations with damping in Section 4.

3 Numerical verification of critical speed model

As a preliminary check of our proposed formulations, we first verify our results with those obtained from a commercially available circular sawing stability code, CSAW[®]. Comparisons are made with frequency-speed diagrams, known as the Campbell diagram. We limit our numerical checks for the case of an unguided saw, and for the case of a guided saw, with the guide modelled as an undamped point spring – since CSAW[®] does not have the facility of including damping. We limit our comparisons for the number of nodal circles, m as 1, and the number of nodal diameters, n as 4. The saw, assumed to be made of steel, is clamped at its inner radius, $r_i = 42.5$ mm, and has a free outer radius, $r_o = 142.5$ mm.

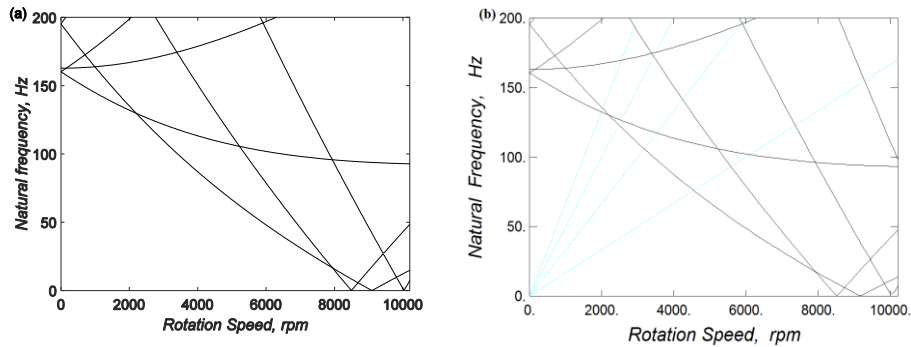


Fig. 2. Campbell diagram for unguided circular saw obtained (a) using analytical model and (b) using CSAW[®].

Campbell diagrams for the unguided case are compared in Fig. 2. As is evident, the critical speed obtained from the proposed analytical model (Fig. 2(a)) occurs at 8497 rpm whereas the critical speed obtained from CSAW[®] (Fig. 2(b)) occurs at 8519 rpm,

which is approximately same as our analytical model. In the Campbell diagram obtained from CSAW[®], there appear four straight lines from the origin. These represent the first four engine order (EO) lines, and correspond to imperfections or unbalance in the rotating parts of the system. These faults generate harmonic and sub-harmonic levels of vibrations [8] as shown in Fig. 2(b).

Campbell diagrams for the guided case are compared in Fig. 3. The guide pad has been modelled as a sector of a circular disc with orientation of inner and outer angle as 5° and 36°, respectively, whereas, inner and outer radius of the guide pad are 57 mm and 142.5 mm, respectively. The spring element, located at the geometric center of the pad, has a stiffness 7.5×10^8 N/m. We observe that the analytical model predicted response (Fig. 3(a)) is consistent with the results from CSAW[®] (Fig. 3(b)), and that there is no change in the critical speed with a single guide. This observation is consistent with those reported earlier in [5].

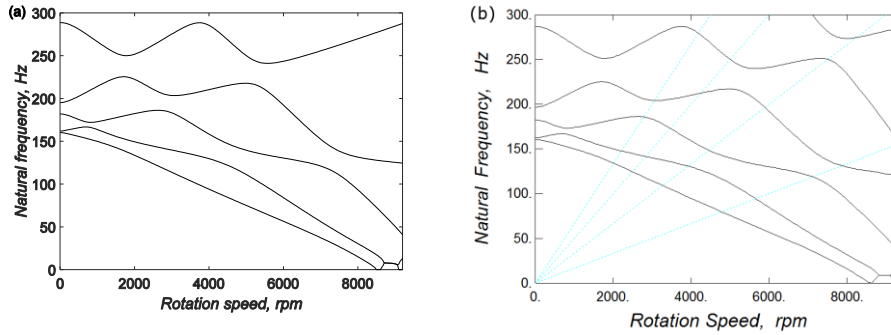


Fig. 3. Campbell diagram for guided circular saw obtained (a) using analytical model and (b) using CSAW[®].

Having numerically verified the analytical model, we use the analytical model to understand how many spring-damper systems are actually necessary to approximate distributed guide and saw interactions, and to understand the role of damping in guides on the critical speeds of circular saws, as is discussed next, in Section 4.

4 Results and Discussion

In this section, we first present convergence analysis for understanding how many spring-damper systems are actually necessary to approximate distributed guide and saw interactions, for a given guide area, followed by analysis for damped guides, followed by analysis on the influence of modelling multiple spring-damper systems radially and circumferentially. Guide pad area for all results presented herein is 4614 mm². Guide location is the same as described in Section 3. All combinations of the spring-damper elements approximating the guide pad are distributed uniformly over the guide pad area. All results presented herein are for the mode corresponding to the first critical speed. All results are presented in the non-dimensional form of the Campbell diagrams.

4.1 Convergence analysis of discrete multiple spring elements to model the guide pad

For a given guide area, and location, it is, in general, difficult to a priori establish the required number of discrete spring elements, necessary to capture the saw and guide interactions. We neglect the damping in the guide presently, influence of which is discussed separately in Section 4.2. We analyze sensitivity of the first critical speed with five combinations of spring elements approximating the same guide area, i.e. with J as 1, 4, 9, 16, and 25. Overall effective stiffness k_j in each case was taken to be as 7.5×10^8 N/m. Results for all cases are shown in Fig. 4.

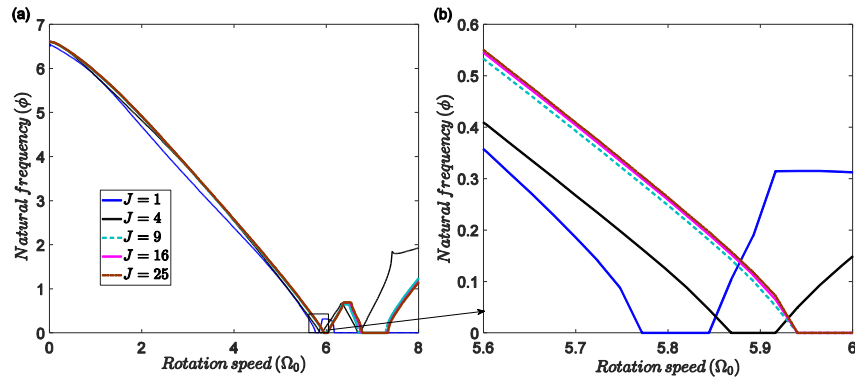


Fig. 4. Campbell diagram for multiple discrete spring elements distributed equally over the guide pad corresponding to the lowest mode

As is evident from the Fig. 4, an increase in number of springs, increases the critical speed. However, beyond 16 springs, the critical speed does not appear to change, suggesting that 16 springs are sufficient to describe the size and location of the guide pad under consideration. Interestingly, we observe that with four discrete springs, the critical speed increases, which is not consistent with the findings reported in [5], in which they found that to increase the critical speed, at least eight discrete uniformly distributed guides modelled as a discrete point spring elements are necessary. This suggests that it is indeed necessary to model the pad-saw interaction as multiple discrete spring elements.

4.2 Influence of damping on the critical speed

Since guides offer not just stiffness, but also damping, influence of damping on the critical speed is reported herein. To delineate the influence of damping, i.e. without stiffness, we present results for a guide with only damping in Fig. 5(a), and for a guide with stiffness and damping in Fig. 5(b). For the case of a guide with damping only, we model the guide to have an overall effective damping of $c_j = 17.2$ N/m/s, for equivalent 16 damping elements. For the case of a guide modelled with discrete spring-damper elements, we take the number of elements to be 16, with an equivalent overall stiffness and damping of 7.5×10^8 N/m and 17.2 N/m/s, respectively.

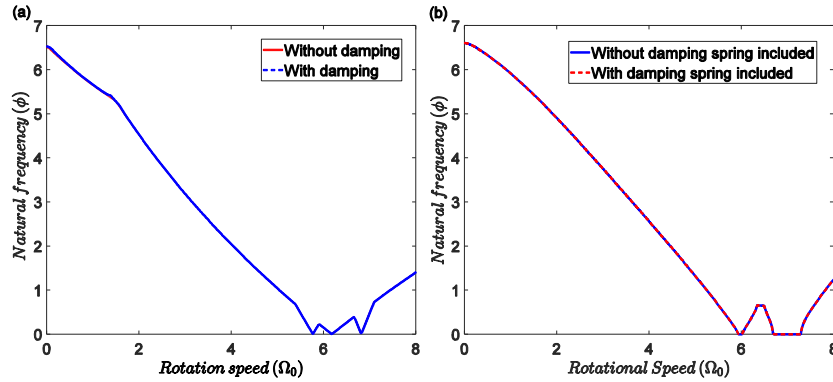


Fig. 5. Campbell diagram for circular saw with pad-saw interaction modelled as (a) discrete damper elements (b) discrete spring-damper elements corresponds to the lowest mode.

As is evident from Fig. 5(a), saws with guides with damping only, i.e. without springs, do not influence the critical speed, and behave like unguided saws, which is curious. We also observe that damping only effects the frequency-speed characteristics. Furthermore, even for the case of guides modelled with multiple discrete spring-damper systems, the critical speed does not change when compared to the critical speed for the case of guides modelled only as springs, as is evident from Fig. 5(b). These observations suggest that damping has no influence on the critical speeds of saws for the given guide pad configuration (mentioned in Section 3), which is unusual and unexpected, and needs further investigations.

4.3 Influence of circumferential and radial distribution of spring elements on the critical speed

In this section, we present the influence of orientation of the distribution of discrete spring elements that are to approximate a given guide pad area, on the critical speed. We present results for the guide pad approximated by different number of discrete spring elements, distributed uniformly in the circumferential and radial directions for a given area. Results for a uniform distribution of discrete spring elements along the circumferential direction (with fixed radial location at 99.75 mm) are shown in Fig. 6, and results for uniform distribution of discrete spring elements along the radial direction (with fixed circumferential location at 20.5°) are shown in Fig. 7. Since damping was shown to not influence the critical speed, we neglect it herein. As before, the overall effective stiffness in each case is taken to be 7.5×10^8 N/m. As is evident from Fig. 6, as the number of discrete spring elements increases along the circumferential direction, the critical speed increases and becomes constant after $J=8$. However, as is evident from Fig. 7, for the case of different discrete spring elements along the radial direction at a fixed orientation, there is no observable change (increase) in critical speed with an increase in the discrete spring elements. We can hence conclude that for a given guide pad area modelled as discrete springs, an increase in discrete spring elements distributed along the circumferential direction leads to an increase in critical speed, whereas

an increase in discrete spring elements distributed along the radial direction does not have any influence on critical speed.

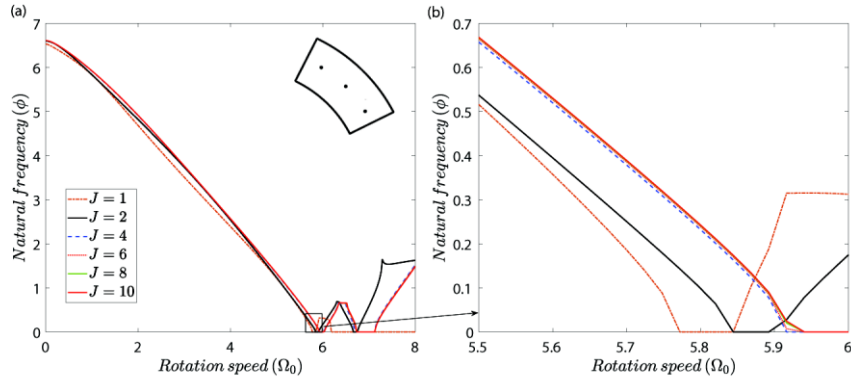


Fig. 6. Influence of multiple spring element over the guide pad in circumferential direction

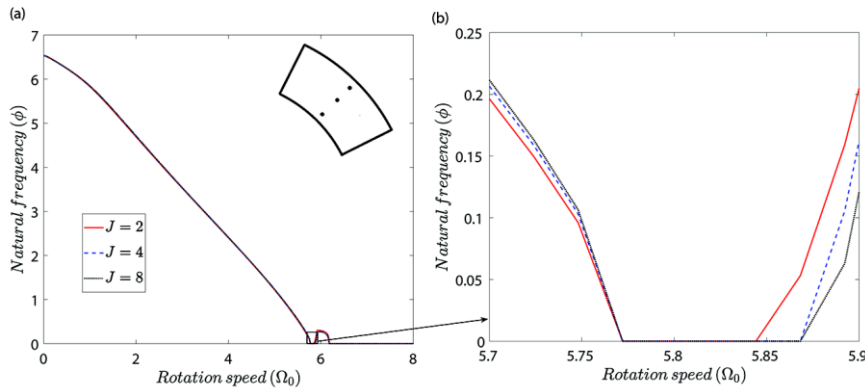


Fig. 7. Influence of multiple spring element over the guide pad in radial direction

These observations, which are different than those observed in the convergence analysis in Sect. 4.1, where we observed the critical speed to not change beyond 16 discrete spring elements approximating the same guide area, suggests that the approach to distributing discrete springs to approximate the guide area has a large bearing on the critical speed. Furthermore, we suspect that these results are not generalizable, but need to be investigated separately for each guide pad area, and location, pointing to the need for a more generalized formulation that models the guide pads as distributed spring-damper systems, rather than multiple discrete spring-damper elements. Further investigations are also necessary to understand how these findings might change for the case of a saw with multiple guides.

5 Conclusion

This paper reports on the influence of guides on the critical speed of rotating saws. Since guides are known to improve critical speeds, understanding how they are modelled is essential to advise guide placement. Using numerically verified analytical models that include guides modelled as multiple discrete spring-damper elements, we observe that damping has no influence on critical speed, which is confounding, and needs further investigations. We also observe that for guides approximated with multiple discrete spring elements, the number, orientation and location of the springs, governs the increase in the critical speed, if any. We observe that for a given guide area, it is necessary to carry out convergence analysis to understand how many discrete spring elements are actually necessary to approximate distributed guide and saw interactions. We also observe that critical speeds are very sensitive to guides modelled with a distribution of discrete spring elements along the radial direction and/or circumferential direction. These observations suggest that a more generalized formulation that models the guide pads as distributed spring-damper systems, rather than multiple discrete spring-damper elements are necessary. Experimental validation is also necessary, and is planned.

Acknowledgements

This research was supported by the Government of India's Science and Engineering Research Board's Early Career Research Award – SERB/ECR/2016/000619.

References

1. G. S. Schajer, "Guided circular saw critical speed theory," Proc. SawTech 1989, Oakland, CA, USA.
2. C. D. Mote and L. T. Nieh, "On the foundation of circular-saw stability theory," Wood Fiber Sci., Vol.-5(2), pp. 160–169, 1973.
3. R. Szymani and C. D. Mote, "Principal developments in thin circular saw vibration and control research," Holz als Roh-und Werkst., Vol.-35, pp. 219–225, 1977.
4. W. D. Iwan and T. L. Moeller, "The stability of a spinning elastic disk with a transverse load system," J. Appl. Mech., Vol. 43(3), pp. 485–490, 1976.
5. S. G. Hutton, S. Chonan, and B. F. Lehmann, "Dynamic response of a guided circular saw," J. Sound Vib., Vol. 112(3), pp. 527–539, 1987.
6. B. F. Lehmann and S. G. Hutton, "Self-excitation in guided circular saws," J. Vib. Acoust. Stress. Reliab. Des., Vol. 110(3), pp. 338–344, 1988.
7. C. D. Mote Jr, "Moving-load stability of a circular plate on a floating central collar," J. Acoust. Soc. Am., Vol. 61(2), pp. 439–447, 1977.
8. A. Mohammadpanah and S. G. Hutton, "Flutter instability speeds of guided splined disks: an experimental and analytical investigation," Shock Vib., Vol. 2015, 2015.
9. G. S. Schajer, "CSAW 4.0 Computer software for optimizing circular saw design," Wood Mach. Institute, Berkeley, CA USA, 2007.
10. P. Hagedorn and A. DasGupta, Vibrations and waves in continuous mechanical systems. John Wiley & Sons, 2007.